Fuel 325 (2022) 124900

Contents lists available at ScienceDirect

Fuel

journal homepage: www.elsevier.com/locate/fuel

Full Length Article

Synthesis of Bio-based oxides nano-composites catalyst from *croton macrostachyus* leaves for biodiesel production from *croton macrostachyus* seed oil

Ramachandran Kasirajan [a,*], Edo Begna Jiru [a], Ermiyas Girma [a], Venkata Ramayya Ancha [b], Sasivaradhan Sadasivam [c], Mani Jayakumar [d,*], Rajasimman Manivasagan [e]

[a] School of Chemical Engineering, Jimma Institute of Technology, Jimma University, Ethiopia
[b] Faculty of Mechanical Engineering, Centre for Environmental Studies, Jimma Institute of Technology, Jimma University, Ethiopia
[c] Faculy of Civil and Environmental Engineering, Jimma Institute of Technology, Jimma University, Ethiopia
[d] Department of Chemical Engineering, Haramaya Institute of Technology/Haramaya University, Dire Dawa, Ethiopia
[e] Department of Chemical Engineering, Faculty of Engineering and Technology, Annamalai University, Annamalai Nagar, Chidambaram, Tamilnadu, India

ARTICLE INFO

Keywords:
Bio-based oxides nano-catalyst
Croton macrostachyus leaves
Non edible seed oil
Biodiesel
Sol–gel process
Ultrasound supported transesterification

ABSTRACT

This study explored the prospective of croton macrostachyus leaves as bio-based minerals rich resource found for metal oxides nano-catalyst synthesis by sol–gel-thermal oxidation method and the seeds as a future lipid-rich non edible resource used for synthesis of biodiesel by ultrasound-supported transeserification process. The prepared catalyst was characterized by diverse analytical practice such as x-ray diffraction (XRD), fourier transform infrared (FT-IR), scanning electron microscopy (SEM), Energy dispersive x-ray (EDX), and Brunauer emmett teller (BET) analysis. The metal oxides nano-catalyst demonstrated very strong basic sites with surface area (126.3 m^2/g), and particle size (23.8 nm) which extensively reduced the diffusion resistance of triglycerides. EDX analysis indicated the presence of Ca-Fe-K-P-Al-Si/C oxides composites was used as nano-catalyst. Maximum yield of 98.85 ± 0.99 wt% achieved with1.23 wt% catalyst, 1:9.13 M ratio of oil to methanol, 36.4085 (round of 36) min reaction period at 50 KHz and 55.48 °C.The oil fatty acid profile and biodiesel were characterized by gas chromatography (GC) and proton nuclear magnetic resonance (^{1}H NMR) spectroscopy, the energy specification of croton macrostachyus biodiesel were analysed and contrasted with ASTM D6751 standard. Nano-catalyst strong basic site enhances the efficiency of biodiesel production.

1. Introduction

Driven by high energy cost, environmental pollution, typical weather changes, an alternative from current petroleum based fossil fuel to a bio-based liquid fuel utilization system is expected to advance progressively and carry a post petroleum era [1–3]. Ethiopia is accomplished with various prospective energy resources like hydropower, solar energy, wind energy and most significantly the biomass energy [4].Comparatively, the biomass based energy has a matchless consideration because the readily available renewable bioresource in huge quantity, which are highly safe and environmental friendly handling resources [5]. Biodiesel is an environment-pleasant fuel, biodegradable, and non-toxic source of liquid energy and it has been produced made by either single or both esterification and/or transesterification techniques [6].

The major familiar approach to produce biodiesel is the route of transesterification reaction process between a source of lipids (fats from animal: dairy fat waste and pig fat, non-edible lipids: crop seeds, plant seeds and algae, municipal waste sludge, yeast lipid & cooked oil waste) and a methyl or ethyl alcohols, predominantly methyl alcohol with the catalyst presence to form methyl esters and glycerol [7–10]. An edible or non edible oils transesterification can be executed using base and/or acidic catalyst [11,12]. The top recognized homogeneous base catalysts for the industrial biodiesel production process are generally used alkaline catalysts such as CH_3ONa, NaOH, KOH for the reason that these have the capable active sites to complete the transesterification reaction within a short time period beneath mild-reaction circumstances. On the other hand, the main inconvenience of homogeneous catalysts are unrecoverable, and non-recyclable, because catalyst separation after the

* Corresponding authors.
E-mail addresses: ramachandran.kasirajan@ju.edu.et (R. Kasirajan), drjayakumarmani@haramaya.edu.et (M. Jayakumar).

https://doi.org/10.1016/j.fuel.2022.124900
Received 29 April 2022; Received in revised form 24 May 2022; Accepted 12 June 2022
Available online 19 June 2022

transesterification reaction is strictly complicated for the reason that the catalyst have been consumed in the reaction and its generate large amount of waste-water, and build severe environmental inconvenience [13–15]. In addition, the function of homogeneous catalytic process in the transesterification reactions very corrosive and enhanced the overall production cost [16] and soap formation, have needs of neutralization & aqueous quench process stages [17,18].

As a result, the inventions of appropriate hetero-catalysts for biodiesel production and other catalytic process (like biocatalyst with multi-hydrolytic from organic waste solid for sludge pre-treatment) from different cheap non-food feedstock are essential to activate the transesterification of oil [19–21]. The hetero-catalysts are separated into the acidic-solid and base-solid in nature catalysts. Countless acidic-solid catalysts were investigated in recent times for biodiesel production and process optimization by esterification and transesterification techniques using inexpensive non-food feed resources [22]. On the other hand, acidic-solid catalysts have some challenges and disadvantages including low surface area, low stabilities, low reactivity, reduced porosity, required excess reaction time and an elevated reaction temperature [23]. In addition, acidic-solid catalysts bear with low amount of acid sites, required large amount of catalyst, leaching of acid sites, deactivation, diffusion-mass transfer limitation, and poisoning due to side reactions. For example, the calcination of acidic nature solid (sulfonated solids) catalysts at a high temperature demolishes catalyst shape, sinking the activity and enhances the process supplementary cost intensive [24].

A base-solid heterogeneous catalyst demonstrates superior catalytic activity than the acidic-solid catalysts. The effectiveness of hetero-base catalysts has been broadly inspected for biodiesel production from diverse resources. Some hetero-base catalysts have been exhibits superior effects, such as hydrotalcites [25], alkaline earth metal oxides [26,27], and alkali earth oxides with alkali metal-doped [28]. Several former hetero-base catalysts have been experienced in transesterification process for biodiesel production which is showing superior catalytic bustle, a few even at lowest thermal condition. This supply's a commercially workable way to reduce production costs for the large scale biodiesel industry. Different researchers have investigated that among hetero-oxides catalysts, CaO rich catalyst has higher efficiency then other catalyst for biodiesel production [29,30]. Efficiency of CaO catalyst have a strong basicity, economically feasible, simple production, and easy to get from natural resources of chicken bone, oyster shell, crab shell, eggshell, snail shell [31]. In previous researcher's investigations, a variety of CaO-based catalysts such as CaO/C, Ni-CaO-montmorillonite, CaO/TiO2, and Li/CaO have been developed and applied for biodiesel production [32].

Nanotechnology used for catalyst synthesis from bio resources has paying enormous attention at present for transesterification of oil [33]. Nano- base catalysts are primed by chemical methods such as chemical vapour, sol–gel, hydrothermal, polyol, and microemulsion & physical method of high energy ball milling, laser pyrolysis, inert gas condensation, pulse vapor deposition and etc. Calcium oxide and calcium rich metal oxides composites were the largely studied catalysts among all basic earth metal oxides for the transesterification reaction to form biodiesel due to its high basic strength, availability, its lesser environmental impact, long catalyst lifetime, and its lower cost which synthesised from waste resources. Croton macrostachyus seed contains rich lipids>50% and its productivity (seed harvesting yearly twice) also meet the requirement of oil demand. The leaves also exhibit minerals rich bio resources. Because of this reason, we selected leaves for nano catalyst preparation and seed as a feedstock for biodiesel production.

In the present research investigation, the total lipids extracted by mixed solvent techniques from *Croton macrostachyus* seeds were utilized as a very cheapest feed resource for synthesis of biodiesel. The physiochemical behaviour of the lipids was examined as per standard scheme. Mainly, a recoverable nano-composite metal oxides catalyst was synthesized from waste bioresource of *Croton macrostachyus* leaves by sol–gel combined with thermal oxidation process as a novel approach. Based on the literature survey, no previous research attempt has been made with the *Croton macrostachyus* leaves for metal oxides nano-catalyst synthesis. The primed nano-catalyst was characterized by SEM-EDX, BET, FTIR, and XRD. In this experimental research, the effects of operational variables for instance catalyst amount, methanol molar ratio with respect to oil, temperature and reaction time at constant ultrasonication frequency of 50 kHz on yield of *Croton macrostachyus* methyl ester. Response surface methodology (RSM) is explored to identify the parameters influence on biodiesel production by transesterification process. Finally, the biodiesel was confirmed by ^{1}H NMR and the properties were categorized by the standard techniques and interacted with ASTM-D6751.

2. Materials and methods

2.1. Materials

The seeds and leaves *croton macrostachyus* was collected from three different places of Jimma, Bedele and Bonga (southwest region) in Ethiopia. Methanol (99.9% purity), hydrochloric acid, sodium hydroxide, hexane (99 % purity), chloroform (99.9% purity) (these chemicals and reagents grade is analytical) have been acquired from sigma-Aldrich, UK.

2.2. Total lipids extraction and characterization

In this research work, three suitable solvents of Hexane: Methanol: Chloroform blends with the ratio of 3:2:1 v/v was used to extract the total lipids present in the Seed [53]. *Croton macrostachyus* seed was initially weighed, and moisture removed with the help of hot oven maintained at 40 °C until removes the bound and unbound moistures, the weight loss of 2.8 wt% was analyzed by gravimetric method. After that, seed was pulverized to obtain uniform size of 0.25 mm for further extraction process. A modified Soxhlet (cylindrical) extractor thimble (500 ml capacity) packed with 25 g of seed was fixed in a flat bottom round shaped flask having the capacity of 500 ml holding, which is the blends of hexane, methanol and chloroform extraction solvent. The other end of the thimble attached with a raw water circulating bulb-condenser to control the solvent vapour loss, converting the vapour into hot liquid and diverting the solvent flow direction towards seed chamber. While the solvents chamber has reached certain level, the chamber was repeatedly drained through a cyclic siphoning action, into the round bottom flask. The cycle was continuously repetitive many times in anticipation of extraction was completed. Properties such as average mean molecular mass, acid content, density, iodine value, free fatty acid (FFA) content, and value of saponification for extracted lipids were analyzed by using standard measures. The compositional fatty acid profiles for the lipids were examined with GC analyzer. 1 g of lipid was injected for analysis and composition profile measurement was carried out with GC, which consisted of column BPX-70 with CHEMIT GC 8610 flame ionization sensing detector. Hydrogen and Nitrogen were used as delivery service gas and the oxygen was used for explosion function. The data was collected with the help of Winchrom software.

2.3. Synthesis of oxides composites nano-catalyst from croton macrostachyus leaves

Calcium rich mineral oxides nano particles were synthesized from powdered *Croton macrostachyus* leaves by sol–gel process procedure. Mineral oxides nano particles preparation by sol–gel was carried out at ambient condition with less energy consumption, and a low cost technique was shown in Fig. 1. Catalyst preparation from waste biological resource was very economical, green, and sustainable [34]. *Croton macrostachyus* leaves based mineral oxides nano-catalyst preparation with constant reaction parameters were conducted as follows:

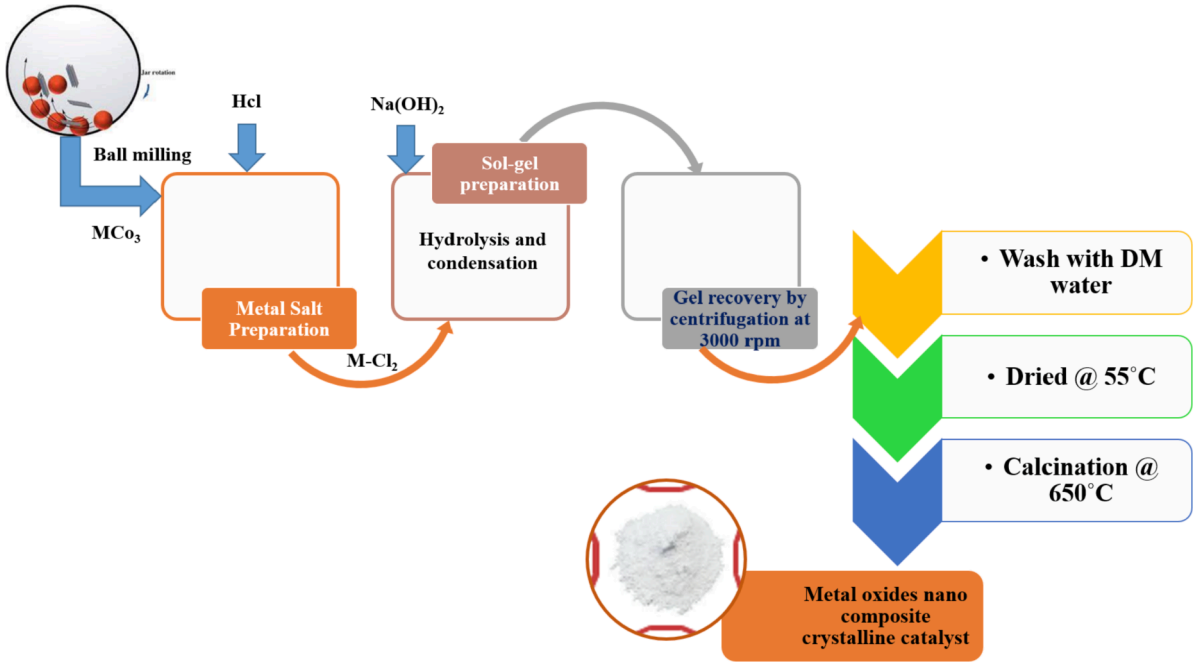

Fig. 1. Catalyst preparation process flow diagram.

Moisture, Lipid content of leaves was separated and the size of the leaves was reduced by rotary ball mill for 12 h to obtain very fine powder. A homogeneous solution of metallic salts, $M-Cl_2$(where M is mixed metals) was developed by dissolved the powdered raw leaves in a dilute HCl. 10.6 g of raw fine powder was dissolved in a 250 ml of 1 M of HCl solution.

$$M-CO_{3\,(s)} + 2HCl_{(aq)} \rightarrow M-Cl_{2(aq)} + H_2O_{(l)} + CO_{2(g)}.$$

Sol was developed by alkaline hydrolysis reaction. The hydrolysis response carries the system more alkaline in an aqueous solution. This approach explored the high ion-exchange capacity. The liquid status colloidal solution prepared using fine solid particles become sol which is nano sized in diameter suspended in a fluid or liquid phase. Metal hydroxyl (M−OH) groups was formed by hydrolysis process, 250 ml, of 1 M concentrated solution of caustic soda drop wise addition was take place into the metallic chloride solution to replace the chloride into the sol at room temperature. The gradual doping of aqueous caustic soda to the sol was generated the precipitation of metal hydroxides and the continuity of addition generates a highly crystalline gel.

$$M-Cl_{2(aq)} + 2Na(OH)_{2(aq)} \rightarrow M\,(OH)_{2\,(s)} + 2NaCl_{(aq)}.$$

Condensation reactions have been used for the formation gel. The condensation reaction takes place while two molecules adhere to create a well-built molecule and liberate a smaller molecule in the course of action. Here the smaller molecules misplaced in the process was sodium chloride. Metal hydroxide gel containing solution was condensed for 24 hrs at ambient condition to condense very well to obtain the gel. After condensation, the $M-(OH)_2$ gel was separated by centrifuge the concentrated solution at 3000 rpm. The gel was cleaned with demineralised water to acquire free of impurities from the precipitate. Then, water was isolated which present in the precipitate and placed in hot air oven to remove the moisture for one day at constant temperature of 55 °C. Finally, the dried powders were calcinated for 1 hr at 650 °C using a furnace and white metal oxides catalyst was obtained in nano sized crystalline [35].

2.4. Characterization of nano-catalyst

The catalyst exterior surface morphological characteristic was studied using SEM analysis for which Helios G4 PFIB CXe equipped with an elevated electrical energy of 10 kV instrument was used. The elemental analysis of catalyst sample was inspected with the attached Bruker-made Energy dispersive X-ray analyzer (EDX). The FTIR spectrometer used for examining the surface functional groups of mixed metal oxides nano catalyst, using a (Perkin-Elmer Inc., USA) Spectrum 100 Fourier transform IR instrument have the widespread equilateral attenuated overall reflectance sample device. In favour of elucidation, infra-red records were composed among the wavelength range of 400 and 4000 cm^{-1}. At last, the correction of an acquired data was implemented by the version of 10.4.2 Perkin-Elmer spectrum software analyzer. The model X'pert Pro was used for segment credentials of mixed metal oxides nano composite catalyst analysis, PAN systematic diffract meter apparatus functioning with Cu-Kα emission supply which have superior scanning accomplished on 2θ array in the rage of 10° to 80° comprises 0.02° as movement range extent. Debye-Scherrer's correlations have been used for the crystalline dimension of mixed metal oxide nano catalyst analysis from the XRD pattern profile. The surface dimensional area and pore size of nano catalyst were characterized using isotherm techniques of nitrogen adsorption followed by desorption at −196° C of liquid nitrogen surrounding temperature with the help of quanta-chrome NOVA2200 apparatus as analyzer for surface. The surface dimensional area has been analyzed using BET theory and the Barrett-Joyner-Halenda (BJH) techniques were used for pore diameter and pore size estimation. First, the impurities present in the samples were removed by degassing process in an oven under vacuum at 383 K for overnight then allowed for nitrogen adsorption followed by desorption isotherm take place under liquid N_2 circumference.

2.5. Biodiesel production process and characterization

A thermostatic ultrasonic probe (model: WS 120040) with an operating frequency of 50 kHz and 1200 W (100%) of operating power was used to perform ultrasonic irradiation. An oil extraction was performed in a modified extractor (soxhlet) with mixed solvents of Hexane, chloroform, and methanol (3:2:1 vol ratio) to achieve higher yield of oil. The extracted Croton macrostachyus crude was blended with demineralised water (3% by volume) and heated to 70 °C, and phosphoric acid 4 wt% added to the mixture. Then, the bleached crude was again blended with 3% demineralised water at constant temperature of 70 °C for 15 min with vigorous mixing. Then, hydrated and non-hydrated gums were

segregated by decantation process which present in the extracted oil. The purified Croton macrostachyus extract placed in oven for the complete water vaporization at 105 °C with gentle mixing to avoid boiled-up [36]. The direct transesterification reaction procedure was performed using refined Croton macrostachyus extract. Purified croton macrostachyus oil taken in a stainless steel flat bottom cylindrical shape (3-necked) reactor with the capacity of 1 litter, the sonic probe fixed in centre neck to maintain uniform distribution of irradiation to the reaction mixtures and this arrangement considered as a biodiesel reactor for the transesterification reaction process. Next, the selected proportions of catalyst and methanol mixtures were filled in the reaction vessel. A cylinder filled with a mixture of reactants and catalysts (oil-methanol-catalyst) have been immersed in an ultrasonic assisted reactor and applied heat to the reaction elevated temperature. Reflux condenser (water-cooled) has been fixed on the reaction vessel side neck, and third neck was used for temperature measurement and sampling during the reaction. For each combination of reactants proportion and process operating conditions, three runs were performed. The complete experimental processes were shown in Fig. 2. After completion of reaction the reactor effluent mixtures centrifuged to recover the nanocatalyst, then decantation was carried out to separate the crude glycerol as bottom by product, the methanol-biodiesel mixture as top product. The rotary evaporation process was used for the recovery of methanol from biodiesel. The recovered methanol and catalyst was reused for further reaction cycle. Hydrogen-1 NMR was used to identify the biodiesel functional group and Croton macrostachyus seed oil converted yield of methyl ester was confirmed using hydrogen-1 NMR spectrum were acquired by Bruker Avance III (500 MHz) device with tetramethylsilane (TMS) as a domestic standard elucidation and $CDCl_3$as a solvent. Hydrogen-1 spectroscopy was validations with pulsation interval of 45 ∘C temperature and 16 scan. From the record of hydrogen-1 NMR spectroscopy, the transesterification yield was deliberated by the Eqn (1).

$$y = \frac{2A_{ME}}{3A_{CH_2}} x100\% \quad (1)$$

Where y - the percentage yield of Croton macrostachyus oil to biodiesel, A_{CH2}–protons of methylene assimilation rate, and A_{ME} - protons of methoxy assimilation rate of the methyl ester. The numerical value of two and three were accounted, commencing the actuality of methylene-carbon acquired two protons, at the same time three protons in methyl alcohol carbons [37]. The properties of cetane number, density, flash point, moisture content, viscosity, and ash content of Croton macrostachyus methyl ester were analysed by means of the method of ASTM standard.

2.6. Experiments design

Based on preliminary final results, we investigated transesterification experiments in Croton macrostachyus seed oil. Process variables affecting the methyl ester production by direct transesterification using mixed metal oxide nano-composite catalyst were developed using variant analysis and surface response methodology (RSM) was used to predict the optimum variable conditions. Therefore, in this investigational task, Design of central composite was particularly used to examine the sound effects of predetermined self-regulating and dependent variables with the response of yield measured in each reaction. The variables that selected for the transesterification reaction are: methanol molar ratio respect to croton seed oil (A), catalyst loading in wt% with respect to oil (B), reaction temperature (C), and the reaction time (D) on Croton macrostachyus methyl eater yield response. Table 1 shows the ranges and level of self-regulating, coded and real value variables selection for Croton macrostachyus seed oil transesterification [38].

Totally thirty experiments were performed individually (6 + 2 k + 2

Table 1
Experimental design for Croton macrostachyus seed oil transesterification at constant ultrasonic frequency (50 kHz).

Operating Variables	Codes	Unit	Levels and Ranges				
			-α	−1	0	+1	+α
Methanol to oil molar ratio	A	mole ratio	3	6	9	12	15
Catalyst loading	B	wt. %	0.5	0.75	1	1.25	1.5
Reaction Temperature	C	°C	35	45	55	65	75
Reaction Time	D	min.	10	20	30	40	50

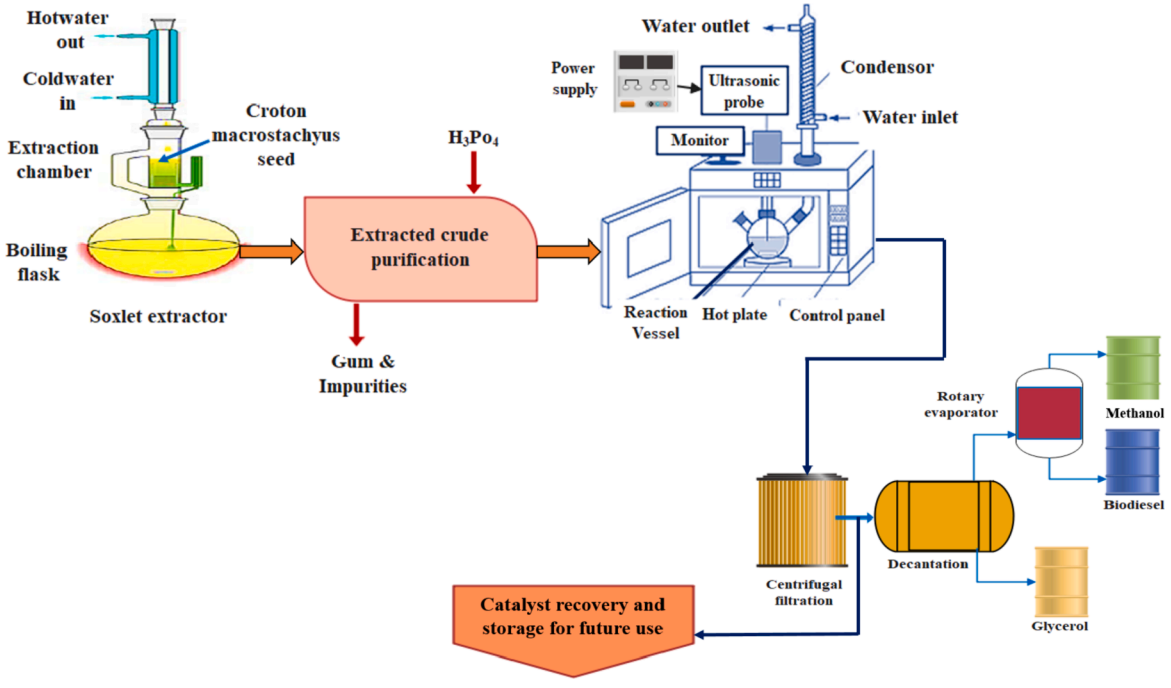

Fig. 2. Process flow diagram of biodiesel synthesis using direct transesterification of croton seed oil.

^{k}), where k is four selected self-regulating variables rooted in 5 level 4 factor comprises 16 (2 ^{k}) factorial point, axial point as 8 and duplicates as 6 at the central point to obtain the investigational inaccuracy [38]. This level selection for each factors were based on the previous research study reports [39–40]. The experimental records achieved from Croton macrostachyus seed oil transesterification process was examined by RSM linear regression testing with CCD design expert 13.0.5.0 version. Statistical investigation gave an experiential regression reproduction of the quadratic polynomial eqn.2. It fits the experimental results and accounts for the effects of linear, quadratic and interactive variables.

$$Y_{ME} = \lambda_o + \sum_{i=1}^{k} \lambda_i x_i + \sum_{j=1}^{k} \lambda_{ii} x_i^2 + \sum_{i=1}^{j-1} \sum_{j=2}^{k} \lambda_{ij} x_i x_j + e \quad (2)$$

Where, Y_{ME} is the biodiesel/FAME yield response factor, λ_o - intercept, λ_i-linear-order coefficient of model, λ_{ii} -factor i^{th} quadratic-coefficient, λ_{ij} - linear mode coefficient intended for relations among i^{th} and j^{th} factors, k - number of parameters selected in this experimental study, x_i and x_j - an self-regulating variables, and e -accidental error.

2.7. Study on stability of catalyst

This investigation examines the stability of recuperated oxides nano-composite catalysts after repeated use in the reaction with/without regeneration. The transesterification setting remains the same as in the previous reaction process, the catalyst was recovered by centrifuge and directly used for another reaction cycle without regeneration, in addition the catalyst is regenerated by washed with methanol to eradicate the precipitates and then it is calcinated in a furnace at 650 °C for one hour. The recuperated oxides nano-composite catalyst was reused under the predicted optimum parameters obtained from ANOVA. The re-usage of the oxides nano-composite catalyst was continued for 6 cycles.

3. Results and discussion

3.1. Characterization of oxides nano-composite catalyst

The SEM and EDX image sol-gelded mixed metal oxides from Croton macrostachyus leaves after calcinations shown in Fig. 3. The texture and surface structure of the oxides nano-composite catalyst was analysed by SEM. The Croton macrostachyus leaves powder particles are normally uneven in nature. Fig. 3 shows that the particles were spongy-like, bubbly and extremely aggregated and assemble together to form lumps of very small particles. The exterior morphology of the catalyst particles shows that the synthesized catalyst dimensions were the lesser in size and therefore the preparation techniques has increased surface porosity with 10 μm magnifications. The lighting part of surfaces from the image exposes large release of electrons when uncovered to the beam of electron. It has shown that large surface dimensional area to capacity ratio in the surface of light parts. Since, it was observed from the micrograph, the synthesized catalysts were made of grains with spherical in shapes agglomerated each other. The small particles agglomerates expose the polycrystalline personality of mixed oxides nano composite. Few of the less significant constituent part emerge to be part mendacious over the top of former constituent part, result the cylindrical nature arrangement. But the image exposed that the most of the synthesized particles are spherical in shape. Other researcher confirmed the spherical shape of NPs [41]. The size of catalyst was reduced after calcination; this because of the alteration of organic molecules throughout calcinations process, or it may be the passing of croton leaves powder through sieves for the separation of larger particles or it may be due to cell wall break during the sol–gel preparation. The surface texture is more or less aggregated crystal small piece with divergent and soft edges linked honestly with one another. In Fig. 4, as agreed that during sol–gel preparation, there are slight of undesirable contaminants presents, as shown in EDX analysis. It causes the dimensional change increment due to agglomeration by the presents of alumina and traces amount of Sodium chloride impurities presents. Table 2 evidently point out the superior composition of O, Ca, and Si, at the same time as Fe is nearby as a transitional element in the composite nano-catalyst. The driven region could be abundant in Si and Ca. There also lowest percent of Al, K, P, and the traces of Cl and Na present in the prepared catalyst. Croton macrostachyus leaves are high in K and C, but at this point their masterpiece is very small, it may perhaps as a result of the EDX spotlight on the Ca, and Si affluent spot, pretty than the K and C affluent-spot. In general, Croton macrostachyus leaves have higher Carbon and potassium content by reason of its organic foundation of C [42].

FTIR spectrum represent in Fig. 5 specify the original bond arrangement after calcinatoin of the nano-composite. Fe-O stretches

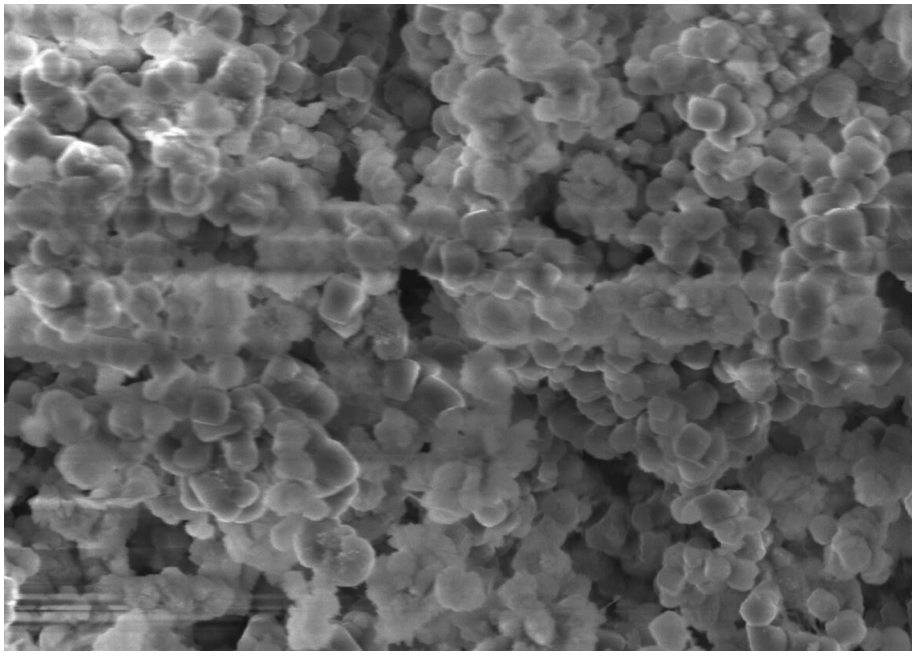

Fig. 3. SEM image of Ca-Fe-K-P-Al-Si/C oxides nano composite catalyst.

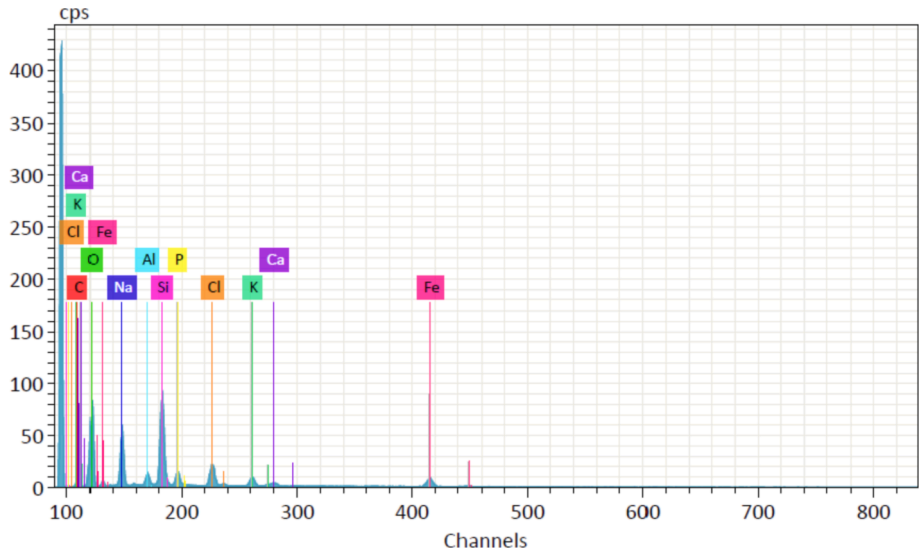

Fig. 4. EDX analysis of Ca-Fe-K-P-Al-Si/C oxides nano composite catalyst.

Table 2
EDX analysis of mixed metal oxides Nanocomposite catalyst.

Elements	Normal Mass %
O	36.63
Ca	20.41
Si	16.41
Fe	13.15
C	5.46
K	3.17
P	1.95
Al	1.38
Cl	0.81
Na	0.63

were attributes at 518 and 714 cm^{-1}, and the Si-O-Si attachment of silicates identified at peak of 1087 cm^{-1} [43], which specifies the existence of silicates among ferrous elements. The peaks at 602 wave number attributes to silica and carbon (Si-C) stretching, the range of 645–715wave number attributable to the stretching of Si-O-Si, and at 460 wave number analogous to pulsation Ca-O-Si from silicate and 752 wave number indicates the stretching pulsation of symmetric Ca-O-Ca [43,45]. Fascinatingly, the original peaks of 600 wave number analogous to C-Si-O, peak at 753 and 972 cm^{-1}analogous to Ca-O(Si) and Ca-O asymmetric extend, respectively. The peaks at 873 and 715wave number may have possibility an exterior plane-flexible pulsation of CO_3 and the interior plane-flexible pulsations of O-C-O, respectively [46,47]. The peaks at 1423 and 1610 cm^{-1} are dispersed to the pulsations of C-O asymmetric attachment in carbonate [48], which validates the calcite associated among ferrous elements as a significant adulteration, and also

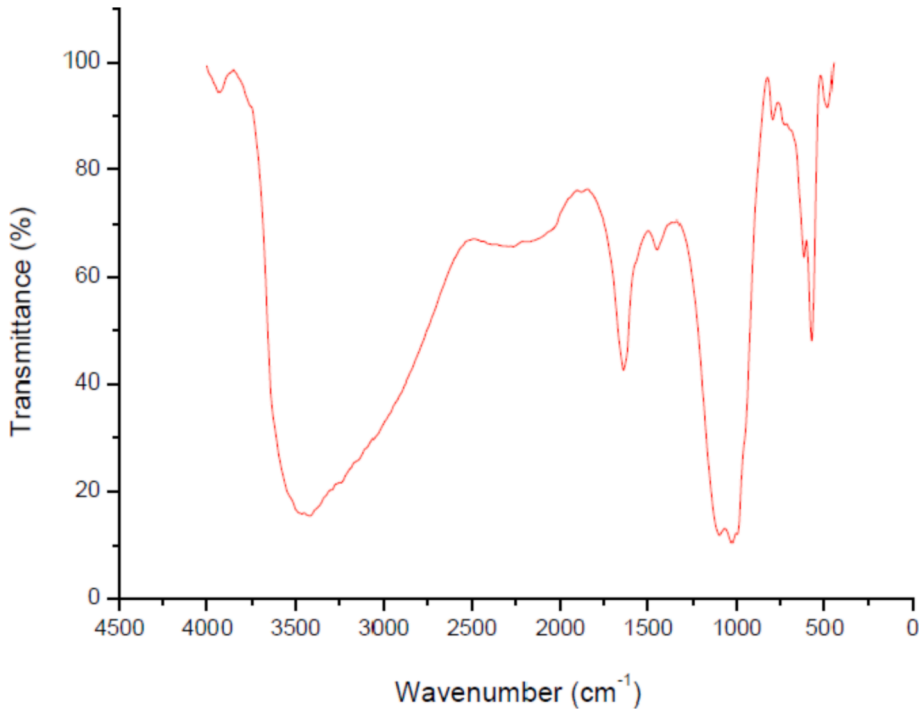

Fig. 5. FTIR analysis of Ca-Fe-K-P-Al-Si/C oxides nano composite catalyst.

validates by SEM-EDX. Yadav et al., also obtained the Analogous by in which they segregates the iron nano-minerals from sacred incense sticks [49].

The XRD prototype shown in Fig. 6 also disclose powerful peak at 34° and 32°, represents the magnetite and haematite segments availability on ferrous particles. A petite peak close to 22° and 26° is an association of quartz and unstructured silica with ferrous elements [50]. The $CaSiO_3$ and Ca-Fe-K-P-Al-Si/C oxides turn out to be more prominent subsequent to sintering at 650 °C, as mounting of sharp at 42° and 47°, correspondingly [44], and are evidently shown in Fig. 6. The peaks at 57° and 76° reveals the carbonates associated with the calcium. The mean particle crystalline size was estimated from the XRD pattern by the Debye-Scherer formula as 23.8 nm.

The particle dimensional values of synthesised catalyst such as surface dimensional area, volume of pore and distribution of pore in size was estimated by nitrogen adsorption followed by desorption techniques are shown in Fig. 7. As the mixed metals loading increase, surface area decreases relative to the silica support. The surface area was found as 126.3 m^2/g by BET theory and by BJH method, the volume of pore and distribution of pore in size was calculated as 58.5 Å and 0.051 cm^3/g, respectively. Surface area shrinkage may be attributed to the catalyst, due to the fact that as the Ca-Fe-K-P-Al species presents in the pores of silica support, there is substantial of the pores and surface coverage. Drop off in the surface area is primary signal of chemical interface among the minerals and silica. The isotherms of N_2 adsorption–desorption reveals that the Ca-Fe-K-P-Al-Si/C oxides are of type IV as per the IUPAC taxonomy and it's demonstrated a H1 hysteresis loop was shown in Fig. 3.

A sharp increase in relative partial pressures from 0.4 and 0.98during adsorption indicates the occurrence of capillary condensation of N_2 in the mesopores, which is attribute the catalyst have the *meso*-porous in nature. Also, significant adsorption amounts specify that there is a substantial volume of nano spaces even after the introduction of Ca-Fe-K-P-Al species in the pores.

3.2. Croton seed and extracted oil characterization

The proximate investigation for seed of Croton macrostachyus was represented in Table 3. From this analysis it was observed that the volatile matter of 86.4%, fixed carbon content as 6.3%, ash content as 4.5%, and moisture content as 2.8% exist. The result showed that the Croton macrostachyus seed's moisture content was within the suggested scale, its contain high volatile substance content of 86.4 percent and low content of ash indicate that highly suitable for fuel production, biodiesel production from the seed oil is effortlessly combustible and the product has neglect able ash content. [51]. Superior wetness presents than the precise scale causes unplanned hydrolysis reaction and deterioration of the lipids for the duration of storage, and increases the expenditure for pre-treatment [52]. Oil was extracted from Croton macrostachyus seed biomass using soxhlet extractor under atmospheric reflux condition with mixed three relative polar solvent system confirmed superior lipid yield. The mixture of three solvents (such as hexane: chloroform: methanol) as 3: 1: 2 ratio (v/v) accomplished higher Croton macrostachyus oil yield from seed. The uppermost oil yield was acquired as 58.6 wt% with most encouraging operation variable conditions of 6:1 solvents to solid ratio (v/w), temperature of 70 °C at atmospheric reflux condition, mean particle dimension of 0.25 mm and90 min of extraction time. R. Kasirajan et al., also stated that lipid extraction from natural plant seed sources by mixed solvent system acquired superior yield which was highly suitable for bio-fuel production [53]. Table 3 shows the average molecular weight of free fatty acids and triglycerides, viscosity, density, acid value, iodine matter, saponification matter, and free fatty acid matter, saturated and unsaturated lipids properties of purified Croton macrostachyus oil. The free fatty acids percent is limited for one step biodiesel production of direct transesterification process as 2.5%. The free fatty acids percent of the purified Croton macrostachyus lipids was observed as 0.6%. Physicochemical properties identification for croton seed extracted oil extremely essential, for the reason that these natures will affect appropriate reaction process parameters, the reaction, selection of the nature of catalyst type, and biodiesel conversion rate and yield [51]. In the straight transesterification reaction process to form biodiesel from fats and lipids, the existence of wetness and free fatty acids constantly result in harmful effects because these combination leads to form soap, consume excess catalyst and shrink the biodiesel production rate [54].The FFAs percent in Croton macrostachyus lipids was very<2.5% of limited value, the acid value also very less as 1.2 mg KOH/g, which permits croton oil as best resource for biodiesel production by a single step direct transesterification reaction. Since the low value of FFAs allowed a base heterogeneous catalytic transesterification reaction process and it has been engaged for the Croton macrostachyus seed oil biodiesel production. Gas chromatography analyzer used for the examination of fatty acids composition and was found as cic-9 oleic acid 27.33%, palmitic acid 25.21%, linoelaidic acid 21.44%, stearic acid 9.5%, *cis*-11eicosenic acid 4.68% and remains are<3% shown in Table 4 and all fatty acids was quantified by relative percentage (w/w). From Table 3, it was observed that the unsaturates (USFAs) where high as 55.97 wt% when contrast with saturates (SFAs) found as 44.03 wt%. From the above analytical examination, we observed that the croton seed oil highly suitable for biodiesel production by direct transesterification process with base catalyst.

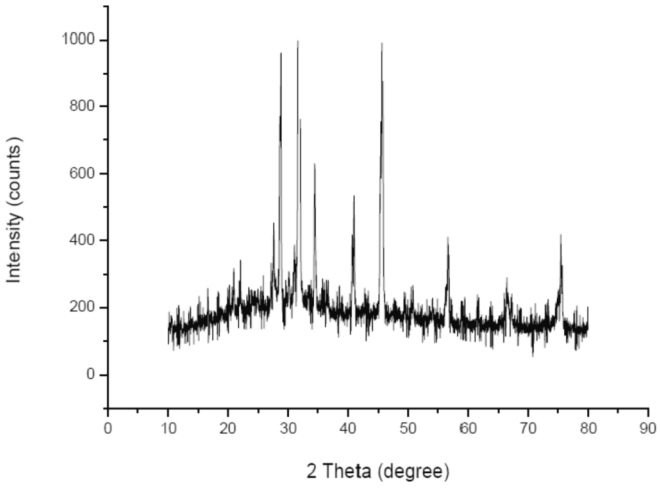

Fig. 6. XRD analysis of Ca-Fe-K-P-Al-Si/C oxides nano composite catalyst.

3.3. Modelling and optimization of transesterification process with Ca-Fe-K-P-Al-Si/C oxides nano composite catalyst by RSM

3.3.1. Analysis of variance (ANOVA)

In the direction of maximize biodiesel production, a comprehensive invent matrix founded on CCD has been used to scrutinize the best arrangement of several operational constraints (methanol mole ration with respect to oil, loading of catalyst quantity, reaction temperature, and time). Table 5 summarizes the complete investigational and projected reply for 30 croton seed oil methyl ester trials with various interaction variables. Advanced multi-regression scrutiny was used to obtain polynomial equation (second order) with deterioration coefficients, which was then examined for algebraic impact. Derived from the ANOVA outcome, RSM software provides four integral replicas to the response: 2 factor interaction (2FI), linear, cubic polynomial, and quadratic. The software recommended a model of quadratic based on the premier polynomial order with added considerable supplementary terms that is not aliased. Eqn.3 represents the finalized model of quadratic regression coefficient founded on coded variables for croton seed oil methyl ester. The significant terms with a positive sign in Eqn.

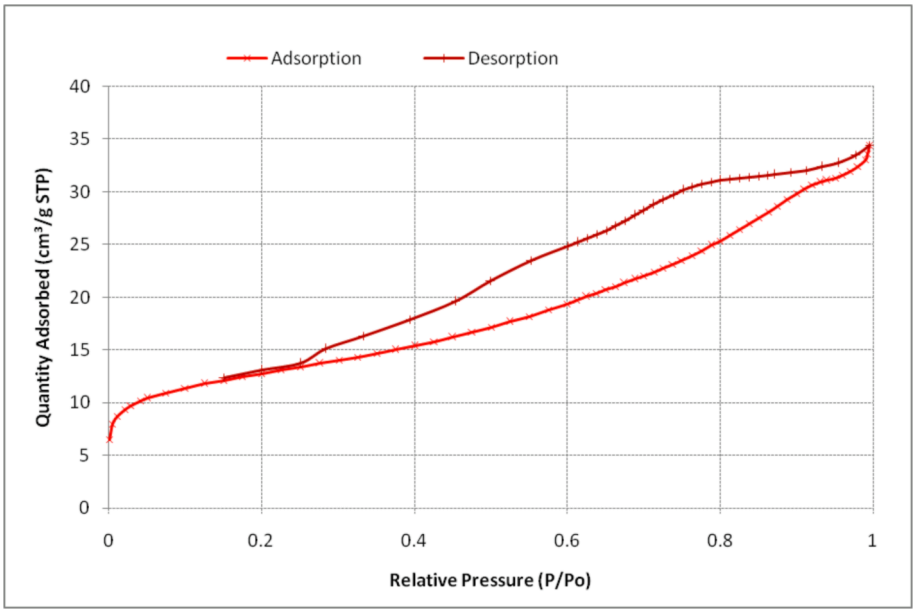

Fig. 7. BET analysis of Ca-Fe-K-P-Al-Si/C oxides nano composite catalyst.

Table 3
Proximate analysis of seed and properties of extracted lipids.

Proximate Analysis of Crotonmacrostachyus seed Contents	Units	values
Volatile matters	%	86.4
Moisture	%	2.8
Ash	%	4.5
Fixed corban	%	6.3
Physicochemical properties of extracted lipids		
Molecular weight of fatty acids	g/mol	280.84
Molecular weight of triglyceride	g/mol	880.58
Density	g/cc	0.891
Viscosity	mm^2/s	43.7
Acid content	mg of KOH/g	1.2
Iodine content	–	89.2
Saponification matter	mg of KOH/g	196.3
Free fatty acid (FFA)	wt%	0.6
Saturated fatty acids (SFAs)	Relative %	44.03
Unsaturated fatty acids (USFAs)	Relative %	55.97

Table 4
Fatty acids composition analysis by gas chromatography [test method: AOAC 996.01 (GLC)].

Fatty acids composition	Carbon atoms	Relative %
Capric	C10:0	1.05%
Palmitic	C16:0	25.21%
Heptadecanoic	C17:0	1.0%
Stearic	C18:0	9.5%
Cis-9 Oleic	C18:1	27.33%
Linoelaidic	C18:2	21.44%
Arachidic	C20:0	1.69%
Cis-11 eicosenic	C20:1	4.68%
Eicosadienoic	C20:2	2.52%
Behenic	C22:0	2.36%
Tricosanoic	C23:0	1.2%
Lignoceric	C24:0	2.02%

(3) indicate a synergistic outcome that significantly persuade the linear outcome to enhance the fatty acid methyl ester content, while the significant terms with a unenthusiastic indication involve an aggressive cause with quadratic conditions that reduce the biodiesel (fatty acid methyl ester) yield.

Table 5
Experimental design and result obtained for Croton macrostachyus seed oil methyl ester (based on CCD).

Run	A: Methano/ Oil molar ratio	B: Catalyst Loading	C: Temperature	D: Time	Yield Response Actual	Predicted
	mol/mol	wt%	°C	min	wt%	wt%
1	12	0.75	45	40	80.3	80.58
2	6	0.75	45	40	71.2	71.01
3	12	1.25	45	40	92.4	92.98
4	9	1	55	30	96.2	95.70
5	6	0.75	65	20	64.8	64.41
6	6	1.25	45	20	77.7	78.16
7	6	1.25	45	40	87.2	87.70
8	12	0.75	45	20	73.5	73.24
9	9	1	55	30	95.4	95.70
10	15	1	55	30	91.2	90.44
11	6	0.75	65	40	76.1	76.30
12	9	1	55	30	95	95.70
13	9	0.5	55	30	58.2	58.88
14	12	0.75	65	40	86.9	86.63
15	9	1	55	10	75.8	75.48
16	9	1.5	55	30	88.9	87.21
17	6	1.25	65	40	92.2	92.64
18	3	1	55	30	73.3	73.04
19	9	1	55	30	96	95.70
20	12	1.25	65	40	97.8	98.67
21	12	0.75	65	20	76.2	76.53
22	9	1	55	30	96.2	95.70
23	6	0.75	45	20	61.9	61.87
24	9	1	75	30	88.2	87.66
25	6	1.25	65	20	79.8	80.35
26	9	1	35	30	79.9	79.43
27	9	1	55	30	95.4	95.70
28	12	1.25	45	20	84.6	85.23
29	9	1	55	50	95.8	95.11
30	12	1.25	65	20	87.8	88.18

$$Yield = 95.7 + 4.35A + 7.08B + 2.06C + 4.91D - 1.07AB + 0.1875AC - 0.45AD - 0.0875BC + 0.1BD + 0.6875CD - 3.49A^2 - 5.66B^2 - 3.04C^2 - 2.6D^2 \quad (3)$$

Table 6 demonstrate an analysis of variance outcome to conclude the

Table 6
Response surface quadratic model-ANOVA forCrotonmacrostachyus seed oil methyl ester based biodiesel.

Source	Sum of Squares	df	Mean Square	F-value	p-value	
Model	3596.58	14	256.90	406.99	< 0.0001	significant
A-Methano/Oil molar ratio	454.14	1	454.14	719.46	< 0.0001	
B-Catalyst Loading	1204.17	1	1204.17	1907.67	< 0.0001	
C-Temperature	101.68	1	101.68	161.09	< 0.0001	
D-Time	578.20	1	578.20	916.00	< 0.0001	
AB	18.49	1	18.49	29.29	< 0.0001	
AC	0.5625	1	0.5625	0.8911	0.3601	
AD	3.24	1	3.24	5.13	0.0387	
BC	0.1225	1	0.1225	0.1941	0.6658	
BD	0.1600	1	0.1600	0.2535	0.6220	
CD	7.56	1	7.56	11.98	0.0035	
A^2	334.00	1	334.00	529.14	< 0.0001	
B^2	880.11	1	880.11	1394.30	< 0.0001	
C^2	253.41	1	253.41	401.47	< 0.0001	
D^2	185.71	1	185.71	294.21	< 0.0001	
Residual	9.47	15	0.6312			
Lack of Fit	8.21	10	0.8208	3.26	0.1023	not significant
Pure Error	1.26	5	0.2520			
Cor Total	3606.05	29				

R^2- 0.9974; Adj R^2 – 0.9949; Predicted R^2 – 0.9864; CV% – 0.9474; Adeq precision – 70.8298.

quadratic model's satisfactoriness and suitability. The regressions model F- value of 406.99 for croton seed oil methyl ester, with 0.0001 as P-value, specifies the replica is highly considerable at the 95 percent of confidence intensity, indicating that the regression model accurately predicts fatty acid methyl ester content. The P-value was accustomed to decide the importance of the model term, with a significance of 0.0001 indicates the source is extremely considerable and a value of > 0.1 indicating that the source is inconsequential. The extremely considerable variables that persuade the methyl ester yield response, according to the ANOVA results, are the methanol to oil molar ratio (A), catalyst loading (B), reaction temperature (C), reaction time (D), and considerable relations panel present among chief factors are: AB, AD, CD, while the considerable quadratic consequence of: A^2, B^2, C^2 and D^2. By comparing the results of predicted outcomes with sensible accurateness of replica to the real time experimental end result using the algebraic technique of appropriate data, the determination value of coefficient (R^2) and determined adjusted-coefficient (Adjusted R^2) reflects the replica dependability. The $R^2 = 0.9974$ and Adjusted $R^2 = 0.9949$ values for croton seed oil methyl ester indicate that the independent variables account for 99.74 percent of the entire variation in biodiesel production. Once the R^2 value is secure to unity of 1, the empirical models fit the experimental data well [55]. The uniformity plot of the actual on the x-axis and anticipated values on the y-axis in Fig. 8 is more rapidly to the tangential line (45°) by means of zero inaccuracy spots. Because these numbers are so secure to the procession of great fit, there is an excellent concurrence among the values of anticipated and experimental, implying that the model is still appropriate. The adequate precision value for croton seed oil methyl ester is 70.83, is > 4 and shows a superior gesture to sound ratio, indicating that this model is desirable. The small coefficient of variation (CV) of 0.9474 percent for croton seed oil methyl ester indicates excellent accuracy and consistency among experimental and projected numerical output values. For croton seed oil methyl ester, the F-value of 3.26 (lack of fit) indicates that this model was not-significant in comparison to the unadulterated error. For the reason that the most important goal was for this model to suit the investigational statistics, a minor lack of fit was most desired.

3.3.2. Independent variables interactive effects analysis by RSM for croton seed oil methyl ester yield

By drawing surface curvature in 3D at the same time trust remaining variables at their middle (0) level, the interactive influence of the independent factors on the proportion of response parameters was explored. In Figs. 9-14, three-dimensional graphs of the biodiesel yield obtained from eqn. (3) in terms of several aspects (Methanol mole ration

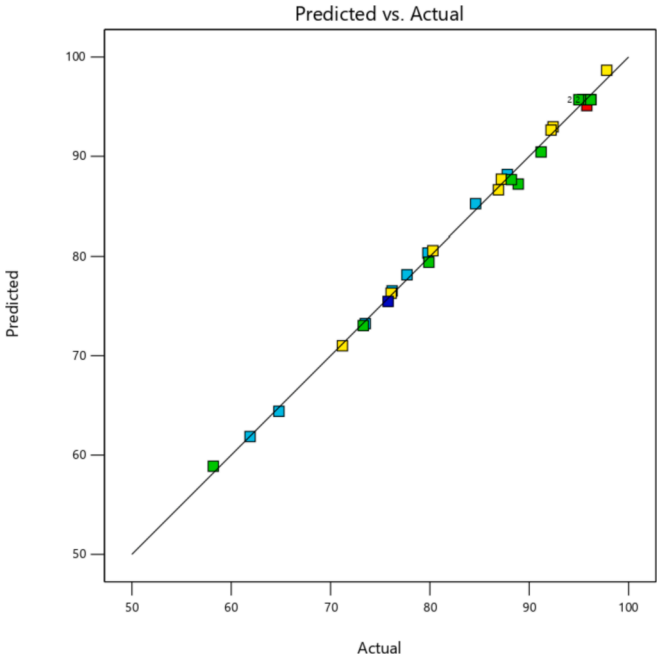

Fig. 8. Predicted versus actual yield of Croton macrostachyus seed oil methyl ester.

with respect to oil, catalyst loading quantity, temperature, and reaction time) were presented. All the trial runs reactions undergoes with the constant ultra-sonication frequency of 50 kHz.

At constant reaction temperature (55 °C) and time, Fig. 9 depicts methanol to croton seed oil molar ratio (A) and loading of catalyst (B) interactive effect on croton seed oil methyl ester yield with 30 min of reaction time. The methyl ester yield enhanced as surplus the molar ratio of methanol to oil and catalyst loading increase. However, because the direct transesterification process is reversible reaction in character, additional requirement of methanol to keep the reactions moving overconfident in order to achieve equilibrium. As the concentration of Ca-Fe-K-P-Al-Si/C oxides nano composite increased with mole ratio, the amount of energetic active sites increased with increased contact among catalyst and reactants, resulting in a superior yield of biodiesel. However, higher catalyst loading dosage supplies to worse the yield of methyl ester due to emulsion configuration, which formulates methyl

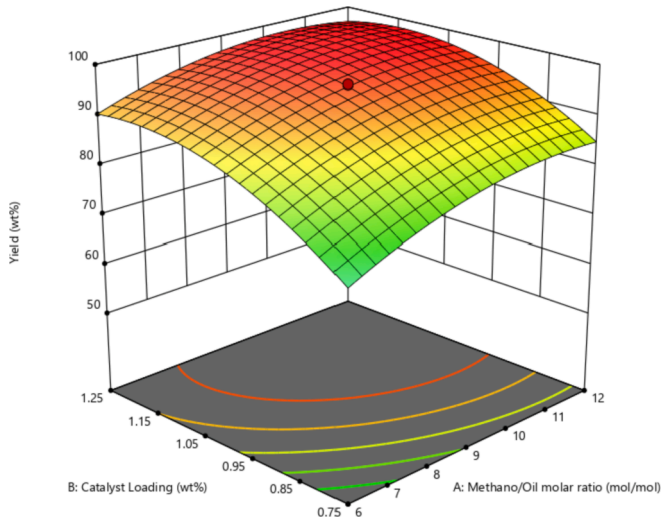

Fig. 9. Catalyst loading and methanol/oil molar ratio interaction effect on yield of croton seed oil methyl ester at constant time and temperature.

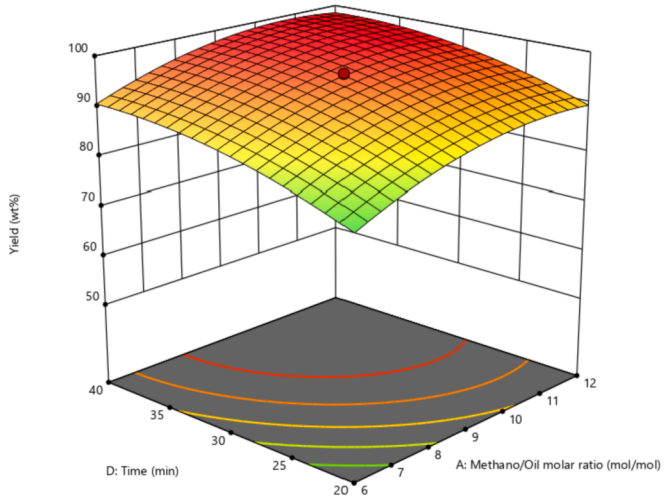

Fig. 10. Reaction time and methanol/oil molar ratio interaction effect on yield of croton seed oil methyl ester at constant catalyst loading and temperature.

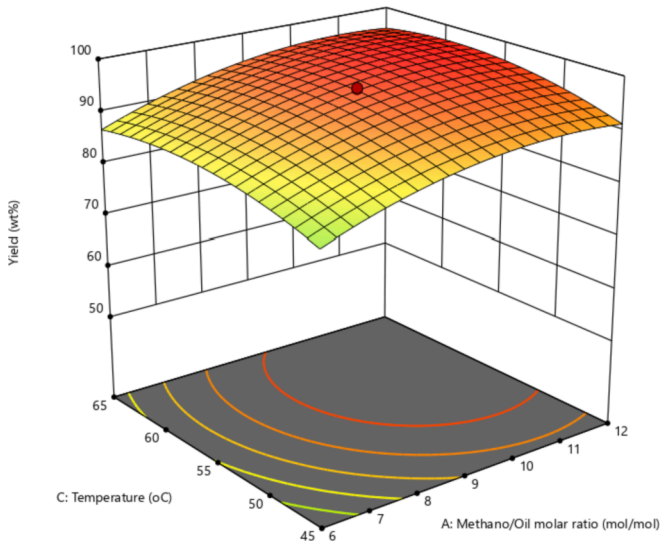

Fig. 11. Reaction temperature and methanol/oil molar ratio interaction effect on yield of croton seed oil methyl ester at constantcatalyst loading andtime.

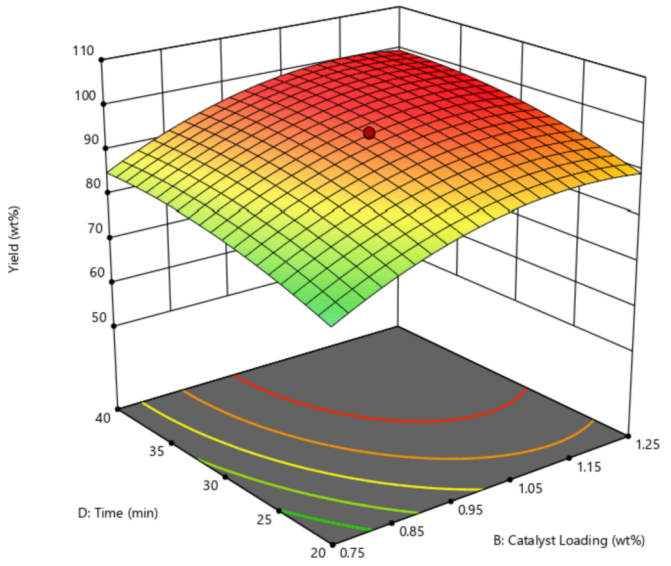

Fig. 12. Reaction time and catalyst loadinginteraction effect on yield of croton seed oil methyl ester at constant methanol/oil molar ratio and temperature.

ester phase partition complex [56–58]. According to ANOVA (Table 6), methanol and catalyst amount interaction effect have the superior significant on methyl ester yield.

The mutual molar ratio of methanol to oil (A) and reaction time (D) effect on croton seed oil methyl ester response is shown in Fig. 10 when catalyst loading quantity (1 wt%) and temperature (55 °C) are held constant. The rate of biodiesel production increases as the direct base catalytic transesterification process reaction progresses. Surface plot revealed that methyl ester yield enhances with mole ratio of methanol to oil and reaction time up to an optimal condition, after which it begins to refuse. Above the constrained optional time, the transesterification reaction process will turn to reverse; lowering the yield of methyl ester and makes phase partition complex [59,60]. From this observation, we bring to a close that the methyl ester synthesis with the time and molar ratio interactive effect is insignificant. The effect of mole ratio of methanol-oil (A) and temperature (C) on croton seed oil methyl ester content was investigated by keeping 1 wt% of catalyst loading (B) and 30 min of reaction time (D) as constant variables, at the same time as the reaction temperature and mole ratio of methanol-oil were varied from lower level and high level, correspondingly. The three-dimensional interaction plot of mole ratio of methanol-oil (A) and temperature (C) in Fig. 11 shows that increasing the temperature increases the yield of fatty acid methyl ester and slightly decreases at higher temperatures (>60 °C), and time causes methanol vaporization, which reduces the yield of methyl ester by reason of decrease in interaction time among oil and methanol [61]. The surface plot revealed that molar ratio and temperature have a minor impact on biodiesel yield.

At constant temperature and mole ratio of methanol-oil (55 °C and 9:1), at the same time as varying quantity of catalyst loading and time between the level ranges of −1 to + 1, the instantaneous confidence of the proportion to croton seed oil methyl ester yield on the relations among catalysts dose (B) and reaction time (D) was studied. The 3D response surface plot in Fig. 12 shows that increasing the catalyst dosage results in a significant increase in croton seed oil methyl ester yield (80 percent to 95 percent) at high levels of reaction time. H.V Lee et al. [62] discovered a similar result, which the highest biodiesel yield is originates at far above the ground level of time. The direct transesterification reaction arrived at equilibrium with higher quantity of catalyst loading and reaction time; however, as the progresses of reaction, the reaction is

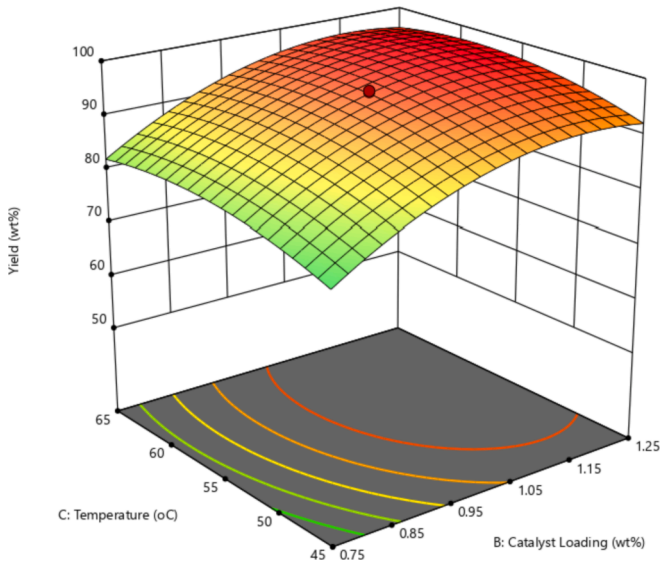

Fig. 13. Reaction temperature and catalyst loadinginteraction effect on yield of croton seed oil methyl ester at constantmethanol/oil molar ratioand time.

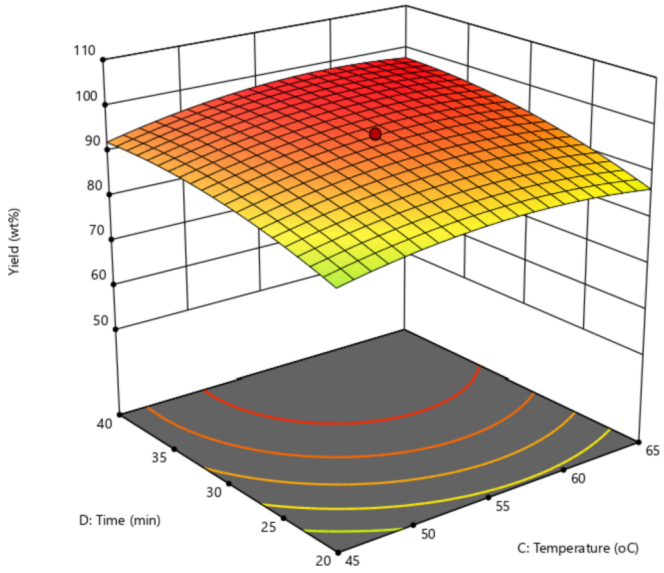

Fig. 14. Reaction temperature and timeinteraction effect on yield of croton seed oil methyl ester at constantmethanol/oil molar ratioand catalyst loading.

reversible, resulting in lower methyl ester substance. In Addition, the yield of FAME decreases at low reaction rates as a result of the mass-transfer diffusion limitation of the Ca-Fe-K-P-Al-Si/C oxides nano-catalyst. The reactive combination system has the three-phase mixture of catalyst-oil-methanol at short reaction time with diffusion constraint, resulting in a slower rate of reaction as a result of oil and methanol immiscibility in nature [63]. Fig. 13 depicts the effect of quantity of catalyst loading (B) and temperature (C) on yield of methyl ester by keeping the reaction time (30 min) and mole ratio of methanol-oil (9:1) as constant. The 3D response plot was changed from low to high (-1 to + 1), which resulted in an increase in croton seed oil methyl ester yield (82 percent to 95 percent). The temperature and Ca-Fe-K-P-Al-Si/C oxides nanocatalyst interactive effect on croton seed oil biodiesel yield is negative (eqn. (3)), indicating that at small levels of Ca-Fe-K-P-Al-Si/C oxides catalyst load, increasing temperature seriously improves yield of biodiesel (up to 55 °C). However, it was discovered that above 1.15 wt % catalyst concentration and temperature above 55 °C, there was a stepwise decline in croton seed oil fatty acid methyl ester yield. This could be for the reason that a high Ca-Fe-K-P-Al-Si/C oxides catalyst amount joint with a higher temperature causes triglyceride side reaction of saponification and the configuration of soaps on reaction blend, its negatively affects the glycerol partition and thus reduces the yield of methyl ester [64]. Other authors [65,66] observed a similar result.

The temperature (C) and time (D) interaction effect on yield of methyl ester in the direct catalytic transesterification process reaction is significant. The croton seed oil conversion to biodiesel is powerfully influenced by reaction temperature and time [58]. The 3D surface plot in Fig. 14 depicts the time and temperature significant interaction effect on the yield of biodiesel, at the same time as keeping the quantity of Ca-Fe-K-P-Al-Si/C oxides catalyst load (1 wt%) and methanol/oil molar ratio (9:1). It's discovered that rising of temperature from a 45 °C to 60 °C resulted in an increase in croton seed oil biodiesel yield with an increase in reaction time. This study found that higher temperatures [>55 °C] result in a lower transesterification rate due to methanol evaporation, resulting in a lower biodiesel yield. Meanwhile, at optimum temperature, catalyst particle dispersion in oil-ester and methanol-glycerol crude medium phases was improved, with enhanced diffusive-mass-transfer among the reactants [66]. According to the plot of curve, at privileged temperatures, the yield of methyl ester was > 92 percent with a range of low to middle level reaction time, which is consistent with other studies [67,68].

3.3.3. *Validation of optimum interacting variables*

To predict maximum biodiesel yield, reaction parameters for direct transesterification catalytic process such as methanol-oil molar ratio (A), catalyst loading (B), reaction temperature (C) and reaction time (D) were optimized with the help of a arithmetical optimization procedure using design expert software version-13.0.5.0. The most favourable process parameters have been set in a ranged coded of −1 to + 1, to achieve the best reaction outcome response for the yield of biodiesel, as shown in Fig. 15.The recommended best possible arrangement of predictor parameters for croton seed oil methyl ester yield was as follows: 9.13:1 Methanol-oil mole ratio, 1.23 wt% of Ca-Fe-K-P-Al-Si/C oxides catalyst quantity, 55.48 °C of reaction temperature, and 36.4085 min of reacting time with a predicted biodiesel yield of 99.84 percent. The precision of forecasted replica is validated by repeating the testing in triplicate under the obtained most favourable operational parameters circumstance, and standard outcome result for the yield of croton seed oil methyl ester are found as 98.85 percent (0.99 percent error). It is possible to conclude that the investigational value obtained with minor inaccuracy revealed an excellent accordance with the forecasted croton seed oil methyl ester yield.

3.3.4. *Stability of croton macrostachyus leaves derived Ca-Fe-K-P-Al-Si/C oxides nano composite catalyst.*

The most essential investigation needs to measure the active site stability and probability of metal based composite nanocatalyst for the production of *croton macrostachyus* biodiesel in huge industrial applications is the reusability of the catalyst. After the first experiment, the Ca-Fe-K-P-Al-Si/C oxides nano composite catalyst was detached from the reactor crude mixture with the help of centrifugal filtration, then the separated catalyst sluiced using methanol, and reused without regeneration. For regeneration, the catalyst was dehydrated in the oven for 12 h at 85 °C, then calcinated for 1 h at 650 °C, and reused. The transesterification process was performed under optimal reaction conditions to interrogate the reusability of catalyst and the outcomes are represented in Fig. 16. The outcome effect showed that as the number of consecutive runs increased, the catalytic activity decreased very fast for the non-regenerated catalyst and the decrement of activity for regenerated catalyst is very low. The yield of methyl ester from croton seed oil was recorded as 81.8 % for the usage of non-regenerated catalyst and 96.6 % for the usage of regenerated catalyst at the 6th cycle, respectively. The activity decline on Ca-Fe-K-P-Al-Si/C oxides nano composite

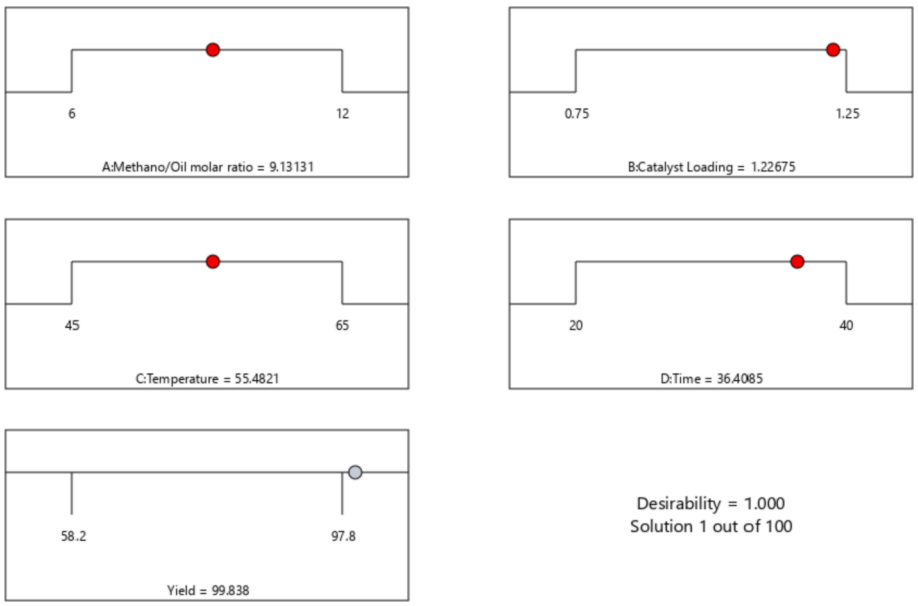

Fig. 15. Desirability ramp for numerical optimization for the selected variables using Ca-Fe-K-P-Al-Si/C oxides nano composite catalyst.

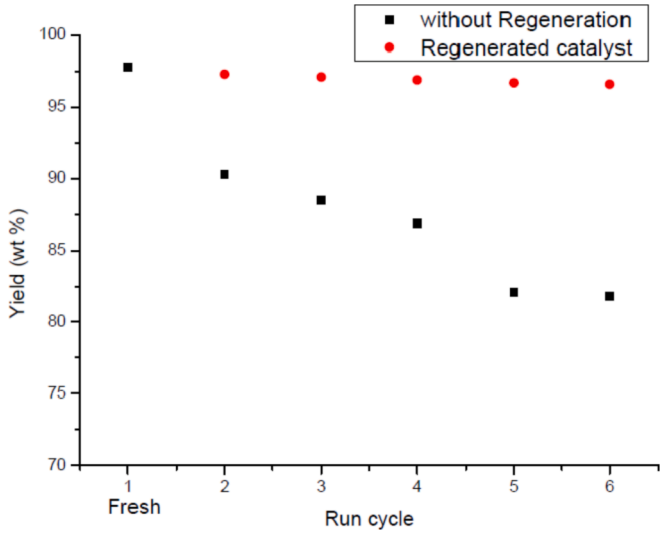

Fig. 16. Stability of Catalyst analysis with and without regeneration.

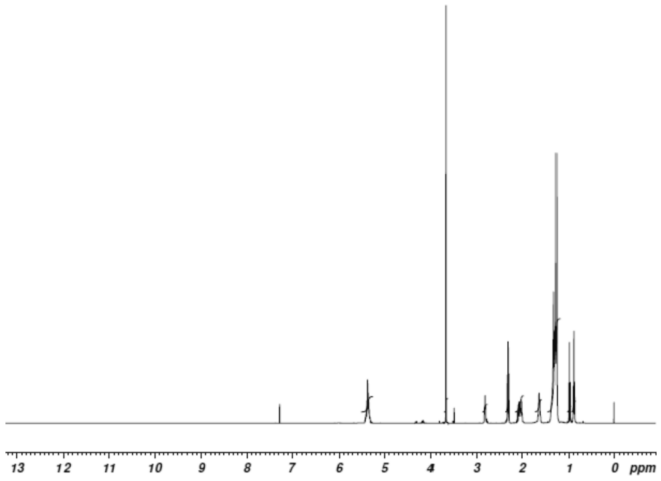

Fig. 17. 1H NMR spectra of Croton macrostachyus seed oil methyl ester.

catalyst is caused by poisoning accumulation over the active sites by layer formation of non reactive oil and glycerol, as well as shrinks the surface dimensional area, volume of pore, and total basicity [69,70]. Also, the leaching of active components from Ca-Fe-K-P-Al-Si/C oxides nano composite catalyst can reduce active site availability on the surface and pores of the catalyst. As a result, the active site discharge for the regenerated catalyst was controlled, and the yield performance was well maintained for each cycle. As a result, with continuous regeneration, the catalyst's stability is maintained and it is possible to reuse the catalyst.

3.4. Biodiesel characterization

The ^{1}H NMR spectra of croton seed oil methyl ester are shown in Fig. 17.The reliability wave formed by the protons of a methyl group (a-CH_2) adjoined to an ester fragment arrangement in triglyceride was solubilised in the peak of 2.3 ppm, whereas the protons present in the methyl ester's methoxy group have been differentiated at 3.66 ppm. Depending on these proton attributes expressions on NMR spectra, biodiesel transformation was confirmed. The methyl ester was successfully converted from croton seed oil and found the yield as97.8 wt%. Table 7 revealed the physic-chemical characteristics of croton macrostachyus biodiesel and it was compared with ASTM and EN standard. The biodiesel produced under optimized condition meet the both standard limit.

4. Conclusion

In this study, the spectrographic properties of synthesised Croton macrostachyus leaves based Ca-Fe-K-P-Al-Si/C oxides nano composite catalyst were investigated, and the results of SEM-EDX, XRD, FT-IR, and BET show a significant use of heterogeneous Ca-Fe-K-P-Al-Si/C oxides nano composite catalyst with 23.8 nm particle size and 126.3 m^2/g surface dimensional area. Response surface methodology used to predict the optimum condition to achieve the highest yield of methyl ester based biodiesel by central composite design for four factors with five levels. A quadratic model with R^2 values of 0.9974 was achieved to find out the yield of croton seed oil methyl ester as a function of process variables. The greatest yield of croton seed oil biodiesel was found as 98.85 ± 0.99 wt% at most favourable process conditions of 9.13:1 mol ratio of methanol-oil, Ca-Fe-K-P-Al-Si/C oxides nanocatalyst loading quantity as

Table 7
Comparison of properties of biodiesel with standardsEN 14214and ASTM D6751.

properties	units	Crotonmacrostachyus biodiesel	EN 14,214	ASTM D6751
Specific gravity	–	0.87	0.86–0.90	0.87–0.90
Viscosity@40 °C	mm^2/s	3.81	3.5–5.0	1.9–6.0
Density	g/cc	0.87	0.86–0.90	0.82–0.90
Calorific value	MJ/kg	41.88	–	–
Flash point	°C	132	≥130	≥120
Cetane number	minimum	54	47	51
Acid matter	mg KOH/g	0.05	≤0.5	≤ 0.8
Free fatty acid	%	0.025	≤0.25	≤0.5
Saponification value	mg KOH/g	174.2	≤218.79	≤215.99
Moisture content	%	0.002	≤0.05	≤0.05
Ash content	%	0.004	≤0.02	≤0.02

1.23 wt%, 55.48 °C of reaction temperature, and 36.4085 min of reaction time. The experimental results fit the statistically estimated model perfectly. Under ideal conditions, the Ca-Fe-K-P-Al-Si/C oxides nanocatalyst can be reused prolong time period with continuous regeneration with neglected loss in biodiesel production. Purified croton seed oil methyl ester fuel properties closely match the biodiesel standards specified in EN 14,214 and ASTM D6751. Accordingly, the methyl ester based biodiesel production from Croton seed extract under appropriate optimum processing conditions can be suggested as a possible fuel source that could supplement hydrocarbon fuel in existing engines, thereby meeting the ever-increasing demand for fuel oil.

CRediT authorship contribution statement

Ramachandran Kasirajan: Conceptualization, Writing – original draft, Methodology, Writing – review & editing, Data curation. **Edo Begna Jiru:** Methodology, Writing – review & editing, Data curation. **Ermiyas Girma:** Methodology, Writing – review & editing, Data curation. **Venkata Ramayya Ancha:** Writing – original draft. **Sasivaradhan Sadasivam:** . **Mani Jayakumar:** Visualization, Investigation, Supervision. **Rajasimman Manivasagan:** Visualization, Investigation, Supervision.

Declaration of Competing Interest

The authors declare that they have no known competing financial interests or personal relationships that could have appeared to influence the work reported in this paper.

Acknowledgement

The authors would like to express our grateful to Centre for ExiST project: Excellence in Science & Technology – Ethiopia (funded by KfW, Germany), this work was financially supported by the Jimma Institute of Technology Center of Excellence-CRGE RESOURCE CART (Climate Resilient Green Economy Resource Centre for Advanced Research and Training—Linking Energy with Water and Agriculture). And the authors extend their sincere gratitude to Centre for excellence Jimma Institute of Technology for their assistance and providing research facility to carry out the present research study.

References

[1] Zhu Z, Xu Z. The rational design of biomass-derived carbon materials towards next-generation energy storage: a review. Renew Sustain Energy Rev 2020;134:110308. https://doi.org/10.1016/j.rser.2020.110308.
[2] Periyasamy S, Karthik V, Senthil Kumar P, Isabel JB, Temesgen T, Hunegnaw BM, et al. Chemical, physical and biological methods to convert lignocellulosic waste into value-added products. A review *Environ Chem Lett* 2022;20(2):1129–52.
[3] Chozhavendhan S, Praveen Kumar R, Bharathiraja B, Jayakumar M. Recent progress on transforming crude glycerol into high value chemicals: a critical review. Biofuels 2016;10:309–14. https://doi.org/10.1080/17597269.2016.1174018.
[4] Berhanu M, Anuradha JS, Kifile Z. Expanding sustenance in Ethiopia based on renewable energy resources e a comprehensive review. RenewSustain Energy Rev 2017;75:1035–45. https://doi.org/10.1016/j.rser.2016.11.082.
[5] Anuradha JS, Lalith D, Prabhu MA, Yimam A, Taye Z. Catalytic conversion of sugarcane bagasse to cellulosic ethanol: TiO_2 coupled nanocellulose as an effective hydrolysis enhancer. CarbohydrPolym 2016;136:700–9. https://doi.org/10.1016/j.carbpol.2015.09.098.
[6] Gardy J, Osatiashtiani A, Céspedes O, Hassanpour A, Lai X, Lee AF, et al. A magnetically separable SO_4/Fe-Al-TiO_2 solid acid catalyst for biodiesel production from waste cooking oil. ApplCatal B Environ 2018;234:268–78.
[7] Selvaganapathy T, Muthuvelayudham R, Jayakumar M, Minar Mohamed Lebbai S, Murugesan MP. Rheological property analysis of pyrolytic liquid fuel (PLF) using ASTM and APHA standards. Mater Today: Proc 2020;26:3030–6.
[8] Selvakumar P, Arunagiri A, Sivashanmugam P. Thermo-sonic assisted enzymatic pre-treatment of sludge biomass as potential feedstock for oleaginous yeast cultivation to produce biodiesel. Renewable Energy 2019;139:1400–11. https://doi.org/10.1016/j.renene.2019.03.040.
[9] Selvakumar P, Sivashanmugam P. Ultrasound assisted oleaginous yeast lipid extraction and garbage lipase catalyzed transesterification for enhanced biodiesel production. Energy Convers Manage 2019;179:141–51. https://doi.org/10.1016/j.enconman.2018.10.051.
[10] Selvakumar P, Sivashanmugam P. Optimization of lipase production from organic solid waste by anaerobic digestion and its application in biodiesel production. Fuel Process Technol 2017;165:1–8. https://doi.org/10.1016/j.fuproc.2017.04.020.
[11] Viola E, Blasi A, Valerio V, Guidi I, Zimbardi F, Braccio G, et al. Biodiesel from fried vegetable oils via transesterification by heterogeneous catalysis. Catal Today 2012;179(1):185–90.
[12] Selvaganapathy T, Muthuvelayudham R, Jayakumar M. Process parameter optimization study on thermolytic polystyrene liquid fuel using response surface methodology (RSM). Mater Today: Proc 2020;26:2729–39. https://doi.org/10.1016/j.matpr.2020.02.572.
[13] Salimi Z, Hosseini SA. Study and optimization of conditions of biodiesel production from edible oils using ZnO/$BiFeO_3$ nano magnetic catalyst. Fuel 2019;239:1204–12.
[14] Liu Y, Zhang P, Fan M, Jiang P. Biodiesel production from soybean oil catalyzed by magnetic nanoparticle $MgFe_2O_4$@CaO. Fuel 2016;164:314–21. https://doi.org/10.1016/j.fuel.2015.10.008.
[15] Jayakumar M, Karmegam N, Gundupalli MP, Bizuneh Gebeyehu K, Tessema Asfaw B, Chang SW, et al. Heterogeneous base catalysts: Synthesis and application for biodiesel production – A review. Bioresour Technol 2021;331:125054.
[16] Osatiashtiani A, Durndell LJ, Manayil JC, Lee AF, Wilson K. Influence of alkyl chain length on sulfated zirconia catalysed batch and continuous esterification of carboxylic acids by light alcohols. Green Chem 2016;18(20):5529–35.
[17] Woodford JJ, Dacquin JP, Wilson K, Lee AF. Better by design: nano engineered macroporoushydrotalcites for enhanced catalytic biodiesel production. Energy Environ Sci 2012; 5(3): 6145–6150.https://doi.org/10.1039/C2EE02837A.
[18] Jayakumar M, Bizuneh Gebeyehu K, Selvakumar KV, Parvathy S, Kim W, KarmegamN. Waste Ox bone based heterogeneous catalyst synthesis, characterization, utilization and reaction kinetics of biodiesel generation from Jatropha curcas oil. Chemosphere 2022; 288: 132534. https://doi.org/10.1016/j.chemosphere.2021.132534.
[19] Selvakumar P, Sivashanmugam P. Multi-hydrolytic biocatalyst from organic solid waste and its application in municipal waste activated sludge pre-treatment towards energy recovery. Process Saf Environ Prot 2018;117:1–10. https://doi.org/10.1016/j.psep.2018.03.036.
[20] Hattori H, Ono Y. Solid Acid Catalysis: from Fundamentals to Applications. 1st ed. CRC Press; 2015.
[21] Lee AF, Wilson K. Recent developments in heterogeneous catalysis for the sustainable production of biodiesel. Catal Today 2015;242:3–18.
[22] Borges ME, Díaz L. Recent developments on heterogeneous catalysts for biodiesel production by oil esterification and transesterification reactions: a review. Renew Sustain Energy Rev 2012;16(5):2839–49.
[23] Ramachandran K, Suganya T, Nagendra Gandhi N, Renganathan S. Recent developments for biodiesel production by ultrasonic assist transesterification using different heterogeneous catalyst: a review. Renew Sustain Energy Rev 2013;22:410–8.

[24] Gardy J, Rehan M, Hassanpour A, Lai X, Nizami A-S. Advances in nano-catalysts based biodiesel production from non-food feedstocks. J Environ Manage 2019;249: 109316.

[25] Reyna VLR, Dias JM, Medellin CNA, Ocampo PR, Martinez RJM, Penaflor-Galindo T, Alvarez Fuentes G. Biodiesel production using layered double hydroxides and derived mixed oxides: the role of the synthesis conditions and the catalysts properties on biodiesel conversion. Fuel 2019; 251: 285–292.https://doi.org/10.1016/j.fuel.2019.03.128.

[26] Pandit PR, Fulekar MH. Egg shell waste as heterogeneous nanocatalyst for biodiesel production: optimized by response surface methodology. J Environ Manag 2017;198:319–29. https://doi.org/10.1016/j.jenvman.2017.04.100.

[27] Çakırca EE, N Tekin G, İlgen O, N Akın A. Catalytic activity of CaO-based catalyst in transesterification of microalgae oil with methanol. Energy Environ 2019;30(1): 176–87.

[28] Malhotra R, Ali A. 5-Na/ZnO doped mesoporous silica as reusable solid catalyst for biodiesel production via transesterification of virgin cottonseed oil. Renew. Energy 2019;133:606–19.

[29] Borah MJ, Das A, Das V, Bhuyan N, Deka D. Transesterification of waste cooking oil for biodiesel production catalyzed by Zn substituted waste egg shell derived CaO nanocatalyst. Fuel 2019;242:345–54. https://doi.org/10.1016/j.fuel.2019.01.060.

[30] Keihani M, Esmaeili H, Rouhi P. Biodiesel Production from Chicken Fat Using Nano-calcium Oxide Catalyst and Improving the Fuel Properties via Blending with Diesel. PhysChem Res 2018;6:521–9. https://doi.org/10.22036/PCR.2018.114565.1453.

[31] Borah MJ, Devi A, Borah R, Deka D. Synthesis and application of Co doped ZnO as heterogeneous nanocatalyst for biodiesel production from nonedible oil. Renew Energy 2019;133:512–9.

[32] Teo SH, Islam A, Chan ES, Thomas Choong SY, Alharthi NH, Taufiq-Yap YH, et al. Efficient biodiesel production from Jatropha curcus using $CaSO_4/Fe_2O_3$-SiO_2 core-shell magnetic nanoparticles. J Clean Prod 2019;208:816–26.

[33] Nizami AS, Rehan M. Towards nanotechnology-based biofuel industry. Biofuel Res J 2018;5(2):798–9. https://doi.org/10.18331/BRJ2018.5.2.2.

[34] Lalit H, Natnael S, Dure M, Thriveni T, Ramakrishna C, Ji WA. Synthesis of nano-calcium oxide from waste eggshell by sol-gel method. Sustainability 2019;11:3196. https://doi.org/10.3390/su11113196.

[35] Nashwan QM, Kalman M, Peter B. Effects of nanocrystalline calcium oxide particles on mechanical, thermal, and electrical properties of EPDM rubber. Colloid and Polymer Sci2021; 299: 1669–1682.https://doi.org/10.1007/s00396-021-04888-5.

[36] Adekunle AS, Oyekunle JAO, Obisesan OR, Ojo OS, Ojo OS. Effects of degumming on biodiesel properties of some non-conventional seed oils. Energy Rep 2016;2: 188–93.

[37] Kasirajan R. Biodiesel production by two step process from an energy source of Chrysophyllumalbidum oil using homogeneous catalyst. SAfr J of ChemEng 2021; 37:161–6.

[38] Mostafaei M, Ghobadian B, Barzegar M, Banakar A. Optimization of ultrasonic assisted continuous production of biodiesel using response surface methodology. Optimization of ultrasonic assisted continuous production of biodiesel using response surface methodologyUltrasonSonochem 2015;27:54–61.

[39] Pandit PR, Fulekar MH. Egg shell waste as heterogeneous nanocatalyst for biodiesel production: optimized by response surface methodology.J. Environ Manag 2017;198:319–29. https://doi.org/10.1016/j.jenvman.2017.04.100.

[40] VermaP, Sharma MP, Dwivedi G. Prospects of bio-based alcohols for Karanja biodiesel production: an optimization study by Response Surface Methodology. Fuel 2016; 183: 185-194.https://doi.org/10.1016/j.fuel.2016.06.062.

[41] MarghiasiZ BakhtiariF, DarezereshkiE EsmaelizadehE. Preparation and characterization of CaO nanoparticles from calcium hydroxide by direct thermal decomposition method. J Ind Eng Chem 2014;20(1):113–7. https://doi.org/10.1016/j.jiec.2013.04.018.

[42] Yadav VK, Gnanamoorthy G, Cabral-Pinto MMS, Alam J, Ahamed M, Gupta N, et al. Variations and similarities in structural, chemical, and elemental properties on the ashes derived from the coal due to their combustion in open and controlled manner. Environ Sci Pollut Res 2021;28(25):32609–25.

[43] Khale D, Chaudhary R. Mechanism of geopolymerization and factors influencing its development: A review. J MaterSci 2007;42(3):729–46.

[44] Ataollahi F, Pramanik S, Moradi A, Dalilottojari A, Pingguan-Murphy B, Wan-Abas WAB, et al. Endothelial cell responses in terms of adhesion, proliferation, and morphology to stiffness of polydimethylsiloxane elastomer substrates. J Biomed Mater Res A 2015;103(7):2203–13. https://doi.org/10.1002/jbm.a.35186.

[45] Lozano-Sánchez LM, Lee S-W, Sekino T, Rodríguez-González V. Practical microwave-induced hydrothermal synthesis of rectangular prism-like $CaTiO_3$. CrystEngComm 2013;15(13):2359.

[46] Kumar RV, Diamant Y, Gedanken A. Sonochemical Synthesis and Characterization of Nanometer-Size Transition Metal Oxides from Metal Acetates. Chem Mater 2000;12(8):2301–5.

[47] Salavati-Niasari M, Sabet M, Fard ZA, Saberyan K, Mostafa Hosseinpour-Mashkani S. Synthesis and Characterization of Calcium Carbonate Nanostructures via Simple Hydrothermal Method. Synth React Inorg Met Nano-Metal Chem 2015; 45(6):848–57.

[48] Balan V, Mihai CT,Cojocaru FD,Uritu CM, Dodi G,Botezat D,Gardikiotis I. Vibrational Spectroscopy Fingerprinting in Medicine: From Molecular to Clinical Practice. Materials 2019; 12(18): 2884.https://doi.org/10.3390/ma12182884.

[49] Gupta N, Yadav VK, Yadav KK,Alwetaishi M,Gnanamoorthy G, Singh B, Jeon BH, Cabral-Pinto MM, Choudhary N, Ali D, Nejad ZD. Recovery of iron nanominerals from sacred incense sticks ash waste collected from temples by wet and dry magnetic separation method. EnvironTechnolInnov 2021, 25, 102150.https://doi.org/10.1016/j.eti.2021.102150.

[50] Dwivedi S, Saquib Q, Al-Khedhairy AA, Ali AYS, Musarrat J. Characterization of coal fly ash nanoparticles and induced oxidative DNA damage in human peripheral blood mononuclear cells. Sci Total Environ 2012;437:331–8. https://doi.org/10.1016/j.scitotenv.2012.08.004.

[51] GubitzGM, Mittelbach M, TrabiM. Exploitation of the tropical seed plant Jatropha Curcas L.BioresourTechnol 1999; 67: 73-82. https://doi.org/10.1016/S0960-8524(99)00069-3.

[52] EvangelosGG, A statistical investigation of biodiesel physical and chemical properties, and their correlation with the degree of unsaturation. Renew Energy 2013; 5: 858-878.https://doi.org/10.1016/j.renene.2012.07.040.

[53] Kasirajan R, Pandian S, Tamilarasan S, Sahadevan R. Lipid extraction from natural plant source of Adenanthera pavonina using mixed solvent by superheated extractor. Korean J Chem Eng 2014;31(3):509–13.

[54] Albuquerque MCG, Machado YL, Torres AEB, Azevedo DCS, Cavalcante CL, Firmiano LR, et al. Properties of biodiesel oils formulated using different biomass sources and their blends. Renewable Energy 2009;34(3):857–9.

[55] Taufiqurrahmi N, Mohamed AR, Bhatia S. Production of biofuel from waste cooking palm oil using nanocrystalline zeolite as catalyst: process optimization studies. BioresourTechnol2011;102 2011;102(22):10686–94.

[56] Shahraki H, Entezari MH, Goharshadi EK. Sono-synthesis of biodiesel from soybean oil by KF/γ-Al_2O_3 as a nano-solid-base catalyst. Ultraso Sonochem 2015;23: 266–74.

[57] LamMK, LeeKT. Mixed methanoleethanol technology to produce greener biodiesel from waste cooking oil: a breakthrough for $SO4^{2-}/SnO_2$-SiO_2 catalyst, Fuel Process Technol 2011; 92: 1639-1645.https://doi.org/10.1016/j.fuproc.2011.04.012.

[58] MaF, ClementsLD, HannaM. The effects of catalyst fatty acids and water on transesterification of beef tallow. Trans Am Soc Agric Eng 1998; 41(5): 1261-1264.

[59] Hsiao M-C, Lin C-C, Chang Y-H, Chen L-C. Ultrasonic mixing and closed microwave irradiation assisted transesterification of soybean oil. Fuel 2010;89(12):3618–22.

[60] Tan KT, Lee KT, Mohamed AR. Production of FAME by palm oil transesterification via supercritical methanol technology. Biomass Bioenergy 2009;33(8):1096–9.

[61] Ong HC, Masjuki HH, Mahlia TMI, Silitonga AS, Chong WT, Leong KY. Optimization of biodiesel production and engine performance from high free fatty acid Calophyllum inophyllum oil in CI diesel engine. Optimization of biodiesel production and engine performance from high free fatty acid Calophylluminophyllum oil in CI diesel engineEnergy Convers Manag 2014;81: 30–40.

[62] Lee HV, Yunus R, Juan JC, Taufiq-Yap YH. Process optimization design for jatropha-based biodiesel production using response surface methodology. Fuel Process Technol 2011;92(12):2420–8.

[63] Semwal S, Arora AK, Badoni RP, Tuli DK. Biodiesel production using heterogeneous catalysts. Biodiesel production using heterogeneous 2011;102(3): 2151–61.

[64] VicenteG, MartinezM, AracilJ. Optimization of integrated biodiesel production. A study of biodiesel purity and yield.BioresourTechnol 2007; 98: 1724-1733.

[65] Ezekannagha CB, Ude CN, Onukwuli OD. Optimization of the methanolysis of lard oil in the production of biodiesel with response surface methodology. Egypt J Pet 2017;26(4):1001–11.

[66] OlutoyeMA, HameedBH. KyMg1-xZn1þxO3 as a heterogeneous catalyst in the transesterification of palm oil to fatty acid methyl esters.ApplCatalA Gen 2009; 371: 191-198.https://doi.org/10.1016/j.apcata.2009.10.010.

[67] PuneetVerma, SharmaMP. Comparative analysis of effect of methanol and ethanol on Karanja biodiesel production and its optimization, Fuel 2016; 180: 164-174. https://doi.org/10.1016/j.fuel.2016.04.035.

[68] Ang GT, Ooi SN, Tan KT, Lee KT, Mohamed AR. Optimization and kinetic studies of sea mango (Cerbera odollam) oil for biodiesel production via supercritical reaction. Energy Convers Manage 2015;99:242–51.

[69] Granados ML, Alonso DM, Sádaba I, Mariscal R, Ocón P. Leaching and homogeneous contribution in liquid phase reaction catalysed by solids: The case of triglycerides methanolysis using CaO. Leaching and homogeneous contribution in liquid phase reaction catalysed by solids: the case of triglycerides methanolysis using CaOApplCatal B 2009;89(1-2):265–72.

[70] Kouzu M, Hidaka J-S. Transesterification of vegetable oil into biodiesel catalyzed by CaO: a review. Fuel 2012;93:1–12.